Current Biology 25, 103–108, January 5, 2015 ©2015 Elsevier Ltd All rights reserved http://dx.doi.org/10.1016/j.cub.2014.11.009

Report

Coherence among Head Direction Cells before Eye Opening in Rat Pups

Tale L. Bjerknes,[1] Rosamund F. Langston,[2] Ingvild U. Kruge,[1] Edvard I. Moser,[1] and May-Britt Moser[1,*]
[1]Kavli Institute for Systems Neuroscience, Norwegian University of Science and Technology, 7489 Trondheim, Norway
[2]Division of Neuroscience, Medical Research Institute, University of Dundee, Ninewells Hospital and Medical School, Dundee DD1 9SY, Scotland, UK

Summary

Mammalian navigation is thought to depend on an internal map of space consisting of functionally specialized cells in the hippocampus and the surrounding parahippocampal cortices [1–7]. Basic properties of this map are present when rat pups explore the world outside of their nest for the first time, around postnatal day 16–18 (P16–P18) [8–10]. One of the first functions to be expressed in navigating animals is the directional tuning of the head direction cells [8, 9]. To determine whether head direction tuning is expressed at even earlier ages, before the start of exploration, and to establish whether vision is necessary for the development of directional tuning, we recorded neural activity in pre- and parasubiculum, or medial entorhinal cortex, from P11 onward, 3–4 days before the eyelids unseal. Head direction cells were present from the first day of recording. Firing rates were lower than in adults, and preferred firing directions were less stable, drifting within trials and changing completely between trials. Yet the cells drifted coherently, i.e., relative firing directions were maintained from one trial to the next. Directional tuning stabilized shortly after eye opening. The data point to a hardwired attractor network for representation of head direction in which directional tuning develops before vision and visual input serves primarily to anchor firing direction to the external world.

Results

Head direction cells are specialized neurons that fire only when an animal faces a certain range of directions in the horizontal plane, independent of the location and speed of the animal [2, 3]. These neurons, which exist in a variety of brain regions [11], are already almost fully developed at the time when animals begin exploring the outside world, at the age of postnatal day 16–18 (P16–P18), a few days after the eyes open at P14–P15 [8, 9]. The present study was designed to determine whether head direction tuning is present at even earlier ages, before the eyelids open and at a time when rat pups still spend nearly all of their time in the nest [12]. We specifically asked whether directional tuning differences are maintained across experiences. If relative firing directions are maintained from one experimental trial to another, before the appearance of vision, it would point to strong innate components in the mechanism for directional tuning in the brain.

A total of 163 cells were sampled from 14 rat pups while the pups moved around twice for 10 min in a circular or square recording box. Eighty-six of these cells were recorded during the last 3–4 days before eye opening; 77 cells were recorded 1–2 days after eye opening. No cells were recorded for more than one block of trials. The total number of recording blocks (sessions) was 57. Pre-eye-opening data were obtained on P11 in one rat, P12 in three rats, P13 in six rats, P14 in eight rats, and P15 in one rat; post-eye-opening data were collected on P14 in one rat, P15 in eight rats, and P16 in eight rats. Individual rats were recorded for 2–6 days. The tetrodes were placed in presubiculum in seven rats, in parasubiculum in four rats, at the border between pre- and parasubiculum in two rats, and in medial entorhinal cortex (MEC) in one rat (Figure 1; Figure S1 available online). The tetrodes were distributed across deep and superficial layers of pre- and parasubiculum and deep layers of MEC. The pups moved freely across the recording arena and covered the entire range of head directions. Median running speeds increased from 7.6 ± 0.1 cm/s before eye opening to 9.4 ± 0.2 cm/s after eye opening (means across animals ± SEM; $t(102) = 6.9$, $p < 0.001$). Mean coverage of the recording box increased from 85.7% ± 0.8% to 91.5% ± 0.8% ($t(102) = 5.0$, $p < 0.001$).

Head-direction-tuned cells were present from the first day when cells could be identified in the target area (P11 and upward; Figures 1 and 2A). To compare directional tuning before and after eye opening, we computed, for each cell, the length of the mean vector for the distribution of firing rates across the 360° of possible head directions. Cells were classified as head direction cells if their mean vector was longer than the 95th percentile of a distribution of mean vector lengths for shuffled firing rates (Figure 2B). Before eye opening, 59 out of 86 cells (68.6%) passed this criterion. After eye opening, 54 out of 77 cells (70.1%) were classified as head direction cells. The percentage of head direction cells was significantly larger than expected by chance for both age groups (large sample binominal test with an expected P_0 of 0.05; pre-eye opening: $Z = 27.1$, $p < 0.001$; post-eye opening: $Z = 26.3$, $p < 0.001$) (Figure 2C). The percentage of head direction cells did not increase from pre-eye opening to post-eye opening ($Z = 0.2$, $p = 0.84$), but their directional tuning improved (mean vector length ± SEM before eye opening: 0.47 ± 0.02; after eye opening: 0.61 ± 0.03; $t(111) = 3.8$, $p < 0.001$) (Figure 2D). The firing rates of the head direction cells did not change significantly from pre-eye-opening to post-eye-opening trials (0.54 ± 0.06 and 0.68 ± 0.09, respectively; $t(111) = 1.3$, $p = 0.20$), but they were lower than in adult animals [8].

Eye opening was accompanied by significant increases in the directional stability of the cells that passed the selection criterion (Figures 2E and 2F). Before eye opening, directional correlations between the first and the second half of the trial were low, with a mean value of 0.24 ± 0.05 ($t(48) = 5.2$, $p < 0.001$). Correlations between trials were at chance level (−0.07 ± 0.04). After eye opening, on P15–P16, the within-trial correlation increased to 0.60 ± 0.05, whereas the between-trial correlation increased to 0.53 ± 0.04. Both increases were significant (within trial: $t(93) = 5.4$, $p < 0.001$, between trial: $t(104) = 10.5$, $p < 0.001$). The increase in stability most likely contributed to the increase in mean vector length in the time-averaged data.

*Correspondence: maybm@ntnu.no

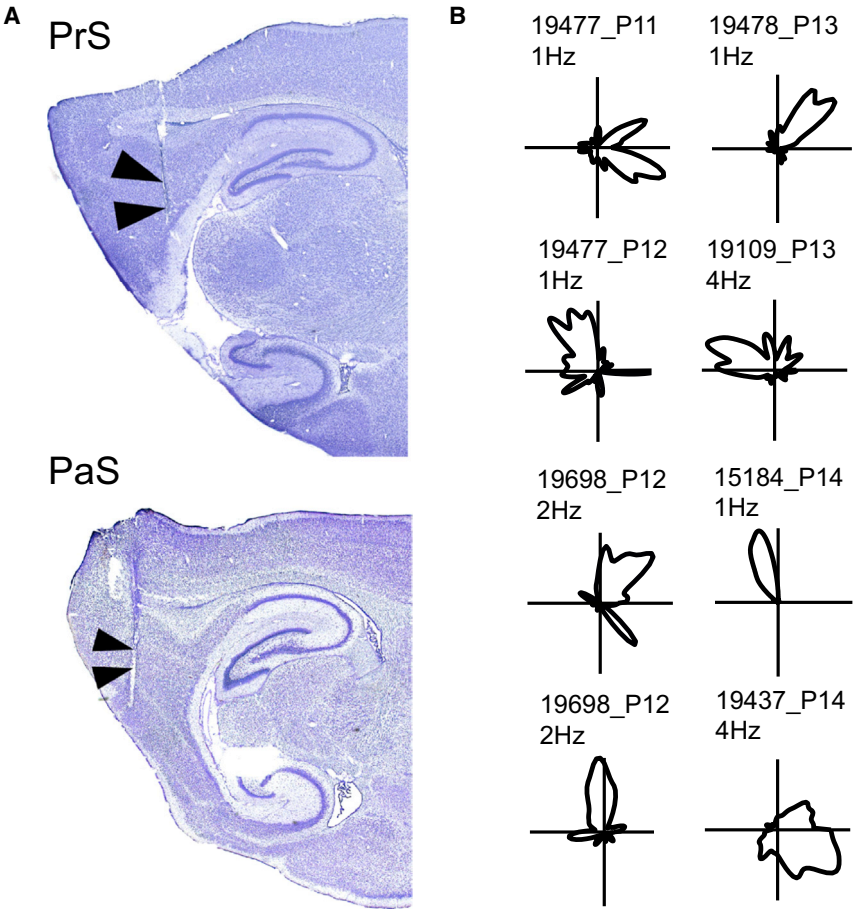

Figure 1. Head Direction Cells Are Present before Eye Opening

(A) Nissl-stained sagittal brain sections with representative recording locations in presubiculum (PrS) and parasubiculum (PaS). See also Figure S1 for recording locations in the remaining animals.

(B) Polar plots showing distribution of firing rate for eight head direction cells recorded before eye opening. Rat number (five digits), postnatal day, and peak firing rate are indicated. All head directions were covered during all recording trials. The low peak rates are representative for the parahippocampal area in this age group [8–10].

After eye opening, directional preferences also rotated along with external cues when the cue card was moved along the wall of the cylinder (Figure S2). During these trials, the cylinder was enclosed by curtains and rotated with the animal out of sight. When the cue card was placed back in the original position, the cells rotated back to the original position.

We asked whether the directional tuning of different cells remained coherent across trials, i.e., if their relative firing directions were maintained, in the presence of the instability in absolute firing directions prior to eye opening. Mean absolute firing directions were calculated for each cell on consecutive trials in which two or more cells passed the 95th percentile criterion for mean vector length. Two or more head direction cells were recorded simultaneously in nine pairs of recording trials (22 cells, 20 cell pairs). The difference between mean firing direction on the first and the second trial was calculated for each cell. The average change in preferred firing direction was 113.1° ± 8.4° (mean ± SEM; Figures 3A and 3B). The change in mean firing directions for individual cells was then compared to the change in relative firing direction for each cell pair recorded on the same two trials, i.e., the change across trials in the angular difference between the mean vectors of each cell pair. In contrast to the absolute changes, the drift in pairwise differences was small (Figure 3A), with a mean value of no more than 20.6° ± 3.6°, clearly lower than the mean for changes in individual cells (comparison of frequency distributions: χ^2 = 37.2, degrees of freedom = 9, $p < 0.001$; Figure 3B versus Figure 3C). The maintained differences in firing direction were also apparent in circular correlations of the angular distribution of firing rate between simultaneously recorded cell pairs. Circular correlations between cell pairs were calculated for each of the two recording trials with at least three simultaneously recorded cells. The directional correlation of a cell pair was highly correlated between trial 1 and trial 2 (data set with ten cell pairs: Pearson product-moment correlation, r = 0.95; data set with three cell pairs: r = 0.79). Thus, even though the head direction cells displayed low stability before eye opening, the ensemble of head direction cells drifted in a coherent manner.

Discussion

These findings show that head direction cells are widely present in parahippocampal areas well before rat pups open their eyes. The directional tuning of these cells is unstable, however, in that peak firing directions drift over the course of minutes in individual trials and change completely between discrete trials. Despite this instability, simultaneously recorded cells maintain relative firing directions, suggesting that a directional map is already present, although anchoring to an external reference frame has not been established.

The fact that cells exhibit directional firing before eye opening is consistent with data from adult animals showing that head direction cells maintain directional tuning in complete darkness even though the preferred tuning direction drifts over extended time intervals [13]. Recordings from adult animals further demonstrate that head direction cells use external visual landmarks to determine firing direction. Rotation of a visual cue card, for example, leads to a corresponding rotation of firing direction on the subsequent trial [14]. The present findings extend these observations by showing (1) that head direction cells develop independently of both vision and outbound navigational experience in young rat pups and (2) that young pups are able to compute instantaneous direction based on integration of angular movement alone. Furthermore, when visual input becomes available at P14–P15, this information is used to calibrate firing direction almost instantly, suggesting that anchoring of directional preferences to the external world can proceed with minimal learning.

The relative independence of vision points to alternative sources of sensory input, such as vestibular information, as

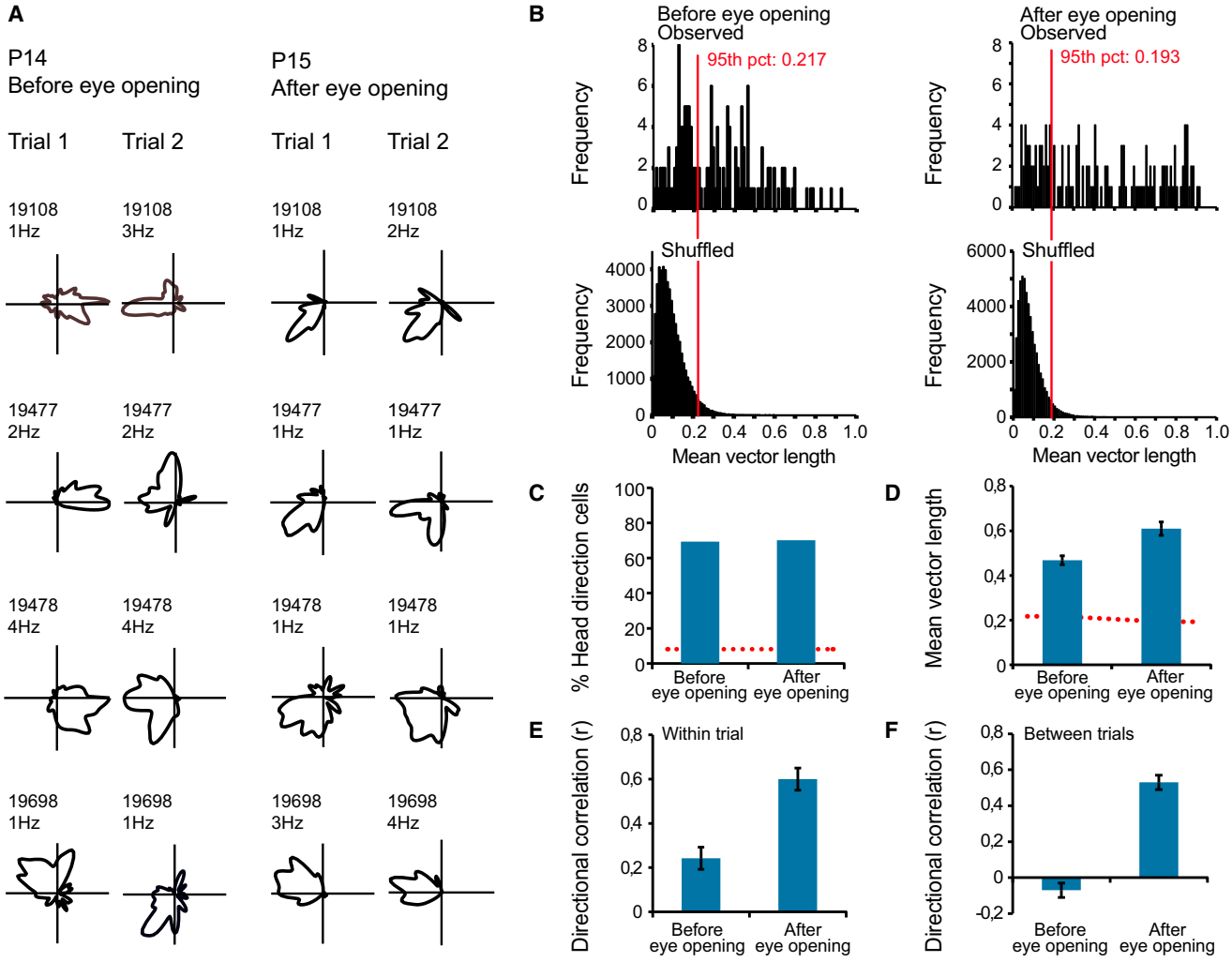

Figure 2. The Effect of Eye Opening on Head Direction Tuning

(A) Four representative head direction cells recorded before eye opening at P14 and four different head direction cells recorded after eye opening at P15 in the same rats. Polar plots for the distribution of firing rate are shown for each cell. Rat number (five digits) and peak firing rate are indicated. All head directions were covered during all recording trials.

(B) Frequency distributions showing mean vector length of firing rate in observed data (top) and shuffled versions of the same data (bottom) before and after eye opening. The red stippled line and the red text indicate the 95th percentile for mean vector length in the shuffled data.

(C) Percentage of head direction cells passing the 95th percentile criterion for mean vector length of firing rate. The red stippled line indicates the upper limit for a 95% confidence interval around the proportion of cells, P_0, expected to pass the 95th percentile criterion by chance (5%).

(D) Mean vector length of firing rate for cells recorded before and after eye opening (mean ± SEM for all head direction cells). The red stippled line indicates the 95th percentile for mean vector length from the shuffled data.

(E) Within-trial directional correlation before and after eye opening (mean ± SEM).

(F) Between-trial directional correlation before and after eye opening (mean ± SEM).

See also Figure S2.

more important for the process of updating firing in head direction cells. In agreement with this possibility, lesions of the vestibular labyrinth or inactivation of the vestibular hair cells disrupt head direction signals in the anterior dorsal thalamic nucleus and the dorsal presubiculum in adult rats [15, 16]. In rat pups, the main features of the vestibular system are in place at an early stage of development. When rat pups are placed on their backs on a surface, for example, they try to right themselves shortly after birth, indicating an early sense of body position [17]. The observation that directional signals emerge before eye opening is consistent with a role for vestibular and other nonvisual modalities in the formation of the head direction signal.

Finally, the coherent drift of head direction cells in rat pups is reminiscent of the maintenance of directional relationships among cell pairs in adult animals [14, 18]. The coherence of the population activity has implications for the developmental mechanism of head direction tuning. Properties of the head direction system have most often been explained by a ring-shaped attractor neural network [19–21], in which cells have strong intrinsic connections that are set up such that only one part of the network is active at any given time. In the presence of sensory inputs, activity in the network shifts along the connectivity ring, in correspondence with movement of the head, and different sets of cells are activated accordingly. Internal coherence would be expected in such a network, even

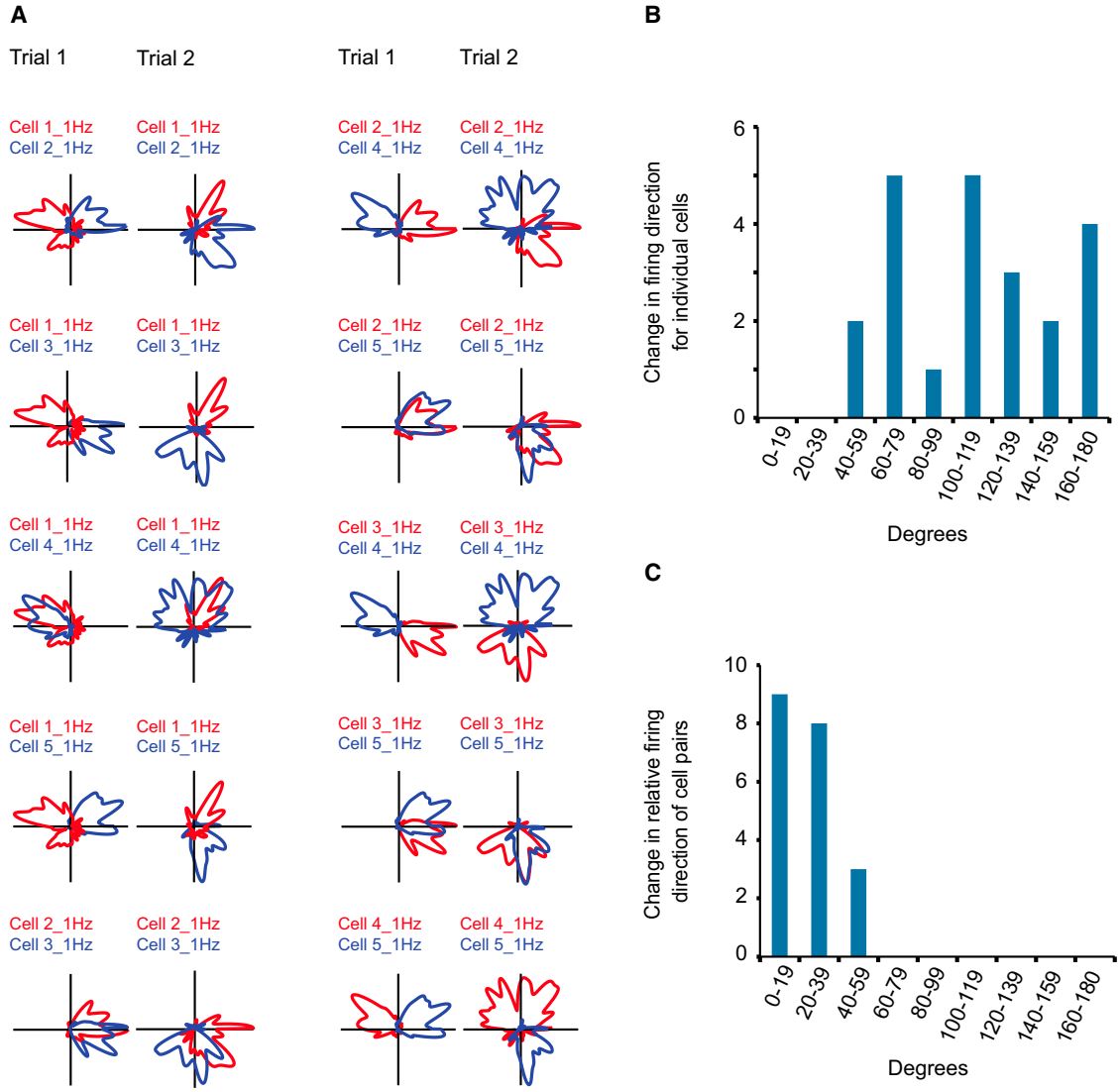

Figure 3. Head Direction Cells Are Unstable before Eye Opening but Maintain Coherence

(A) Polar plots showing distribution of firing rate for ten pairs of head direction cells from a single experiment before eye opening. One member of the pair is shown in red, the other in blue. Cell number (1–5) and peak firing rate are indicated for each cell. All head directions were covered during all recording trials. Note that cells are unstable between trials yet rotate in a coherent manner.

(B) Change in mean firing direction across trials for individual cells. The analysis includes all cells that were recorded simultaneously with one or several other head direction cells on two consecutive trials before eye opening.

(C) Change in relative firing direction (angular difference) across trials for all pairs of head direction cells recorded on two consecutive trials. Low values imply that relative firing directions are maintained.

in the absence of external sensory signals, and therefore these data support such a model.

Experimental Procedures

Subjects

A total of six male and eight female juvenile rats were used for the experiments. Post-eye-opening data from three of the rats were included in a previous study [8]. The pups lived with their mother and siblings in transparent Plexiglas cages in a temperature- and humidity-controlled vivarium less than 30 m from the recording arena. The animals were kept on a 12 hr light/12 hr dark cycle and had free access to food and water throughout the experimental period. All rats were bred in the laboratory. Pregnant mothers were checked multiple times per day between 8 a.m. and 8 p.m. P0 was defined as the first day a new litter was observed. The size of the litter did not exceed eight pups.

The pups' eyelids were checked before every recording session. Recordings were obtained from ten rats before their eyes opened at P14–P15. When a slit between the eye lids was observed on one or both sides, the pup was left in the cage until both eyes had a clear opening. Recordings were then continued and placed in the post-eye-opening group. Each animal was tested over a period of 2–6 days between P11 and P16.

Surgery

Rat pups were implanted between P10 and P14. On the day of surgery, the rats were anesthetized in an induction chamber with 5% isoflurane and 2000 ml/min room air. After induction of anesthesia, the rat was secured in a stereotactic frame, the air flow was reduced to 1,200–1,600 ml/min, and isoflurane was gradually reduced to 0.5%–1.0%. The rat received a subcutaneous injection of bupivacaine (Marcaine) near the incision site and carprofen (Rimadyl) as a general analgesic. Each rat was implanted with a miniature microdrive with two tetrodes aimed at pre- or parasubiculum.

The tetrodes were made of 17 μm platinum-iridium wire cut flat to the same level. The tetrodes were platinum plated to reduce impedances to approximately 200 kΩ at 1 kHz. Coordinates for the tetrode tips were 3.3–3.5 mm lateral from the midline, 1.5–1.8 mm in front of the transverse sinus, and 2.0–2.5 mm ventral to the dura. A jeweler's screw was anchored to the skull as a ground electrode. Depth of anesthesia was monitored using tail and pinch reflexes and by observation of the animal's breathing. Shortly after surgery, the pup was placed back with its mother and siblings. Rats were extensively handled to ensure that pups with implants were accepted upon return to the cage.

Data Collection

The data collection started the day after surgery. The rat pup rested on a flower pot covered with a towel while the signal was checked. The pup was connected to an eight-channel light-weight counterbalanced cable connecting the implant to a computer through an AC-coupled unity-gain operational amplifier. The recorded signal was band-pass filtered between 0.8 and 6.7 kHz and amplified 6,000 to 14,000 times. Recorded spikes were stored at 48 kHz with a 32 bit time stamp. A camera in the ceiling tracked the positions of two light-emitting diodes (LEDs) placed on the head stage. The diodes were positioned 3.5 cm apart and aligned transversely to the animal's body axis.

Tetrodes were lowered in steps of 25–50 μm until single neurons were identified. When the signal exceeded approximately four times the noise ratio, the rat pup was placed in a small cylinder (50 cm diameter, 50 cm height) and was allowed to explore freely for two consecutive trials of 10 min each. The rat rested in the flower pot, on a pedestal, between the trials (5–15 min). Two rats were run in a 50 cm × 50 cm square enclosure (50 cm height) for a similar duration. The walls of the arenas were covered with black adhesive plastic with a prominent white cue card (25 cm × 50 cm) placed centrally on one side. The oldest rats (P15–P16) were given chocolate or vanilla biscuit crumbs to enhance motivation. Most rats were tested two times per day for 3–4 days. Intertrial intervals were 2 hr or more. After the recording session, the tetrodes were generally moved further, and new cell clusters were obtained. The pups were warmed by handling before and after recording to prevent temperature loss.

In a subset of animals in the post-eye-opening group, an additional trial was recorded in which the cue card in the recording arena was shifted 90° clockwise. In this trial, the recording arena was enclosed by black curtains so that no distal cues were visible.

Analysis of Spike and Position Data

Cell identification was done manually using a graphical cluster cutting tool, with 2D projections of the multidimensional parameter space consisting of waveform amplitudes. Autocorrelations and cross-correlations were used as additional separation tools. Putative interneurons were identified using amplitude width and firing rate as criteria. Interneurons were not included in further analyses. The position of the LED pair on the rat's headstage was tracked by an overhead camera. Epochs in which the animal ran less than 2.5 cm/s or more than 100 cm/s (tracking artifacts) were removed from the data set. The remaining position data were smoothed using a 21-sample boxcar window filter (400 ms, ten samples on each side).

Analysis of Head Direction Cells

The head direction of the rat was monitored for each tracking sample by plotting of the relative positions of the two LEDs onto the horizontal plane. A directional tuning function was then generated for each cell by plotting of the firing rate as a function of the rat's directional heading. Only cells with more than 80 spikes and an average rate of more than 0.2 Hz were included in the analyses. Maps for spike frequency and time were smoothed prior to statistical analysis and graphical presentation with a 1D Gaussian kernel with a SD of 6°.

The directional tuning of each cell was expressed by the length of the mean vector of the circular firing-rate distribution. Head direction cells were defined as cells with mean vector lengths above the chance level, estimated for each age group by a shuffling procedure. For each of the 400 permutations of the shuffling procedure, the entire sequence of spikes fired by the cell was time-shifted along the animal's path by a random interval between 20 s and the total trial length minus 20 s, with the end of the trial wrapped onto the beginning. A polar firing-rate map was then constructed, and the mean vector length was determined. A distribution of mean vector lengths was then generated for the entire set of permutations from all cells in the sample, and the 95th percentile was determined. Head direction cells were identified as cells in which the mean vector length exceeded the 95th percentile of the shuffled distribution. The stability of direction-tuned cells was evaluated by correlation of either the spikes in each half of a trial (within-trial stability) or the spikes of two consecutive trials (between-trial stability). Cells were only included in analyses if the rat had moved its head through all four directional quadrants.

Histology and Reconstruction of Recording Positions

Tetrodes were not moved after the last recording day. The rat received an overdose of pentobarbital and was perfused with an intracardial injection of 0.9% saline followed by 4% formaldehyde. The brain was stored in 4% formaldehyde for at least 48 hr. After this, the brain was quickly frozen and cut in 30 μm sections. The slices were mounted on glass and stained with cresyl violet. The final position of the tip of each tetrode was identified on digital pictures of the brain sections.

Approvals

Experiments were performed in accordance with the Norwegian Animal Welfare Act and the European Convention for the Protection of Vertebrate Animals Used for Experimental and Other Scientific Purposes. The experiments were approved by the National Animal Research Authority of Norway.

Supplemental Information

Supplemental Information includes two figures and can be found with this article online at http://dx.doi.org/10.1016/j.cub.2014.11.009.

Author Contributions

T.L.B., R.F.L., E.I.M., and M.-B.M. planned experiments and analyses, T.L.B., R.F.L., and I.U.K. collected data, T.L.B. and R.F.L. analyzed data, and T.L.B., E.I.M., and M.-B.M. wrote the paper, with input from the other authors.

Acknowledgments

We thank V. Frolov and R. Skjerpeng for programming; M.P. Witter for advice on histology; and A.M. Amundsgård, K. Haugen, E. Henriksen, K. Jenssen, E. Kråkvik, B.B. Løfaldli, and H. Waade for technical assistance. This work was supported by the Kavli Foundation, a student research grant from the Faculty of Medicine at the Norwegian University of Science and Technology, an Advanced Investigator Grant from the European Research Council ("ENSEMBLE," grant agreement 268598), and Centre of Excellence and FRIPRO grants from the Research Council of Norway.

Received: October 14, 2014
Revised: November 5, 2014
Accepted: November 5, 2014
Published: November 26, 2014

References

1. O'Keefe, J., and Dostrovsky, J. (1971). The hippocampus as a spatial map. Preliminary evidence from unit activity in the freely-moving rat. Brain Res. *34*, 171–175.
2. Ranck, J.B. (1985). Head direction cells in the deep cell layer of dorsal presubiculum in freely moving rats. In Electrical Activity of the Archicortex, G. Buzsáki and C.H. Vanderwolf, eds. (Budapest: Akademiai Kiado), pp. 217–220.
3. Taube, J.S., Muller, R.U., and Ranck, J.B., Jr. (1990). Head-direction cells recorded from the postsubiculum in freely moving rats. I. Description and quantitative analysis. J. Neurosci. *10*, 420–435.
4. Hafting, T., Fyhn, M., Molden, S., Moser, M.B., and Moser, E.I. (2005). Microstructure of a spatial map in the entorhinal cortex. Nature *436*, 801–806.
5. Solstad, T., Boccara, C.N., Kropff, E., Moser, M.B., and Moser, E.I. (2008). Representation of geometric borders in the entorhinal cortex. Science *322*, 1865–1868.
6. Lever, C., Burton, S., Jeewajee, A., O'Keefe, J., and Burgess, N. (2009). Boundary vector cells in the subiculum of the hippocampal formation. J. Neurosci. *29*, 9771–9777.
7. Moser, E.I., Roudi, Y., Witter, M.P., Kentros, C., Bonhoeffer, T., and Moser, M.B. (2014). Grid cells and cortical representation. Nat. Rev. Neurosci. *15*, 466–481.

8. Langston, R.F., Ainge, J.A., Couey, J.J., Canto, C.B., Bjerknes, T.L., Witter, M.P., Moser, E.I., and Moser, M.B. (2010). Development of the spatial representation system in the rat. Science *328*, 1576–1580.
9. Wills, T.J., Cacucci, F., Burgess, N., and O'Keefe, J. (2010). Development of the hippocampal cognitive map in preweanling rats. Science *328*, 1573–1576.
10. Bjerknes, T.L., Moser, E.I., and Moser, M.B. (2014). Representation of geometric borders in the developing rat. Neuron *82*, 71–78.
11. Taube, J.S. (2007). The head direction signal: origins and sensory-motor integration. Annu. Rev. Neurosci. *30*, 181–207.
12. Loewen, I., Wallace, D.G., and Whishaw, I.Q. (2005). The development of spatial capacity in piloting and dead reckoning by infant rats: use of the huddle as a home base for spatial navigation. Dev. Psychobiol. *46*, 350–361.
13. Goodridge, J.P., Dudchenko, P.A., Worboys, K.A., Golob, E.J., and Taube, J.S. (1998). Cue control and head direction cells. Behav. Neurosci. *112*, 749–761.
14. Taube, J.S., Muller, R.U., and Ranck, J.B., Jr. (1990). Head-direction cells recorded from the postsubiculum in freely moving rats. II. Effects of environmental manipulations. J. Neurosci. *10*, 436–447.
15. Stackman, R.W., and Taube, J.S. (1997). Firing properties of head direction cells in the rat anterior thalamic nucleus: dependence on vestibular input. J. Neurosci. *17*, 4349–4358.
16. Stackman, R.W., Clark, A.S., and Taube, J.S. (2002). Hippocampal spatial representations require vestibular input. Hippocampus *12*, 291–303.
17. Altman, J., and Sudarshan, K. (1975). Postnatal development of locomotion in the laboratory rat. Anim. Behav. *23*, 896–920.
18. Yoganarasimha, D., Yu, X., and Knierim, J.J. (2006). Head direction cell representations maintain internal coherence during conflicting proximal and distal cue rotations: comparison with hippocampal place cells. J. Neurosci. *26*, 622–631.
19. Skaggs, W.E., Knierim, J.J., Kudrimoti, H.S., and McNaughton, B.L. (1995). A model of the neural basis of the rat's sense of direction. Adv. Neural Inf. Process. Syst. *7*, 173–180.
20. Redish, A.D., Elga, A.N., and Touretzky, D.S. (1996). A coupled attractor model of the rodent head direction system. Netw. Comput. Neural Syst. *7*, 671–685.
21. Zhang, K. (1996). Representation of spatial orientation by the intrinsic dynamics of the head-direction cell ensemble: a theory. J. Neurosci. *16*, 2112–2126.

Current Biology, Volume *24*

Supplemental Information

Coherence among Head Direction Cells before Eye Opening in Rat Pups

Tale L. Bjerknes, Rosamund F. Langston, Ingvild U. Kruge, Edvard I. Moser, and May-Britt Moser

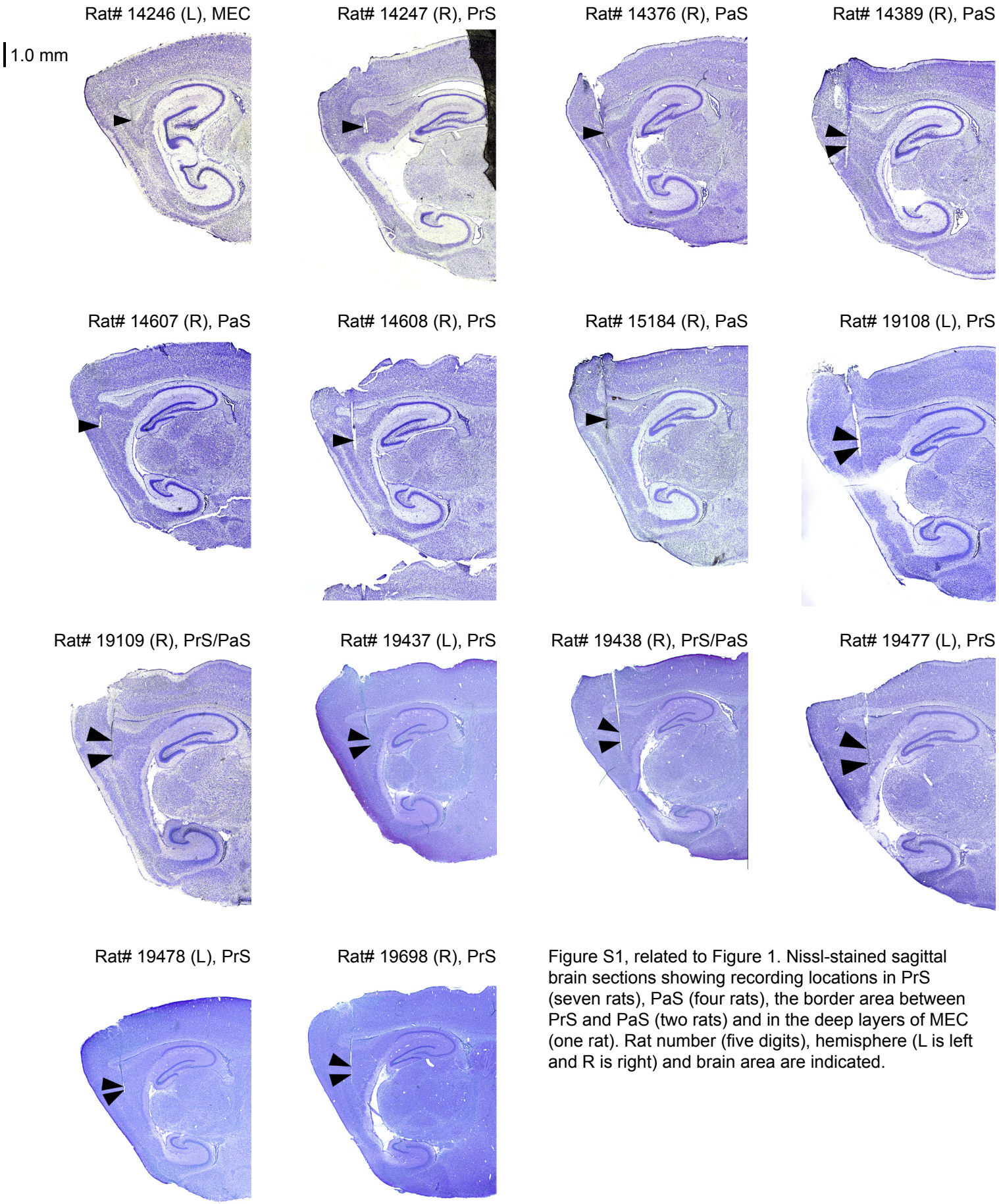

Figure S1, related to Figure 1. Nissl-stained sagittal brain sections showing recording locations in PrS (seven rats), PaS (four rats), the border area between PrS and PaS (two rats) and in the deep layers of MEC (one rat). Rat number (five digits), hemisphere (L is left and R is right) and brain area are indicated.

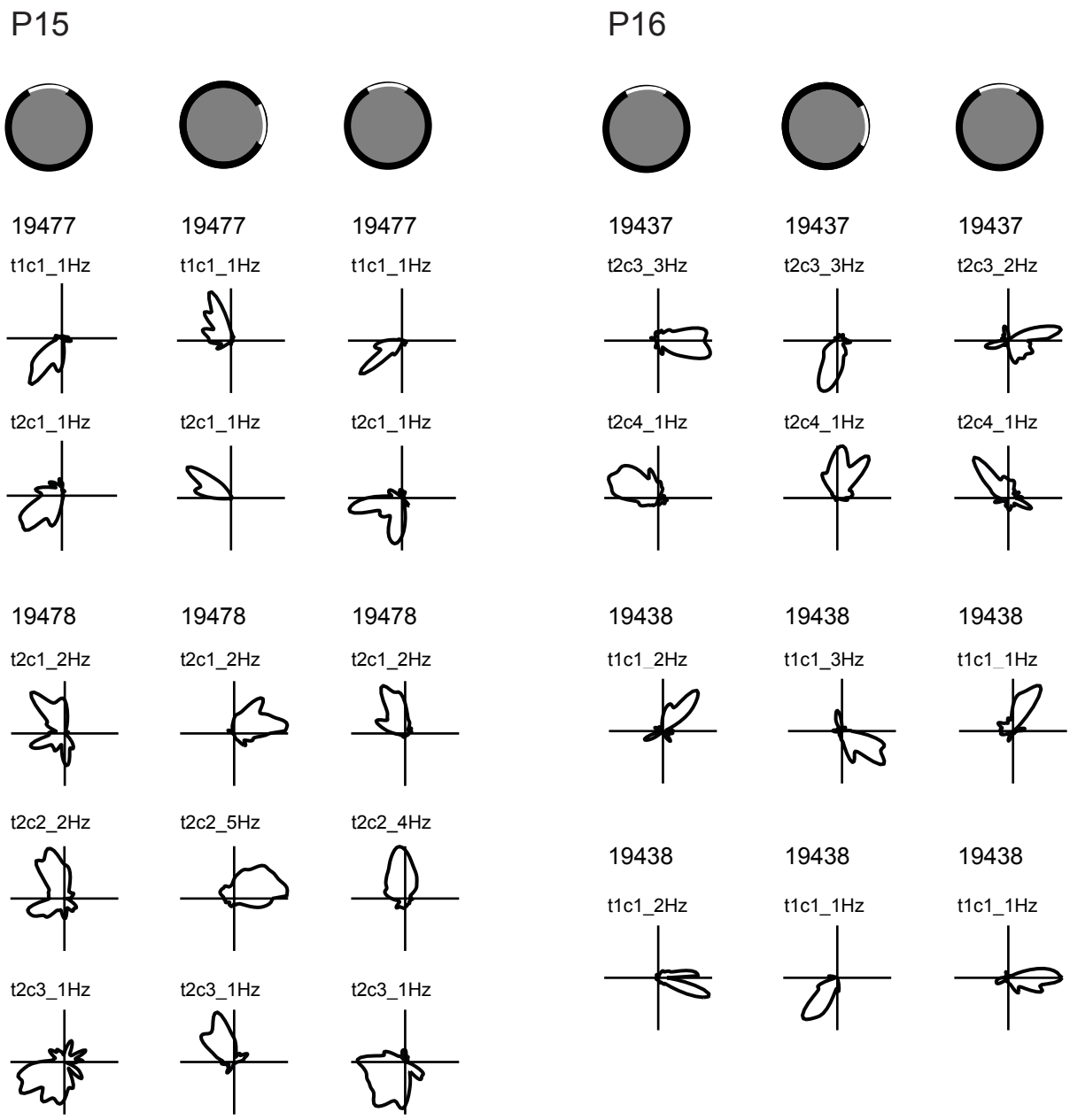

Figure S2, related to Figure 2. Visual cue-based rotation of head direction cells shortly after eye opening. Examples of three consecutive trials where the cue card in the recording arena was rotated 90 degrees clockwise in the middle trial. Schematic at the top shows position of cue card. Directional rate distribution is shown for 5 head direction cells from P15 and 4 head direction cells from P16. Rat number (five digits) is indicated for each set of trials. Cell number (t = tetrode, c = cell), and peak firing rates are indicated above each cell. All head directions were covered during all recording trials.